ISSN (E): 2959-3921
(P): 2959-393X
DOI: https://doi.org/10.59122/144CFC16

Ethiopian International Journal of Engineering and Technology (EIJET)
Volume 1, Issue 2, 2023

Pulmonary Disease Identification and Classification using a Deep Learning Approach

Minalu Chalie[1*] and Zewdie Mossie[1]

[1]Department of Information Technology, Debre Markos University, Ethiopia

[*]Corresponding Author's Email: minaluchal@gmail.com

Abstract

Deep Learning (DL) models have shown strong results in detecting diseases from medical images. In this paper, we explored the challenge of classifying pulmonary diseases (PD) using chest X-rays. The research focuses on three common respiratory conditions: pneumonia, pulmonary tuberculosis, and pleural effusion. We proposed a new framework for detecting and classifying PD from chest X-ray (CXR) images. The process includes noise reduction, image enhancement, data augmentation, segmentation, feature extraction, and classification. To remove noise, we used a Gaussian filter, and for improving image quality, we applied an advanced histogram equalization method. The Region of Interest (ROI) of the lungs was extracted using Otsu's threshold segmentation technique. For feature extraction, we used the Gabor filter to obtain texture details from the images. A Deep Convolutional Neural Network (DCNN) was then used for classification. The system classifies images into four categories: normal, pneumonia, pulmonary tuberculosis, and pleural effusion using a four-way SoftMax classifier. We tested four DCNN models: VGG16, VGG19, ResNet50V2, and DenseNet201. Among these, DenseNet201 performed best, achieving a training accuracy of 97.80% and a testing accuracy of 95.73%. Compared with other advanced models, DenseNet201 showed higher accuracy and better capability in detecting and classifying pulmonary diseases.

Keywords: Feature Learning, Gabor Filter, Pulmonary Disease, Segmentation, X-Ray, Respiratory Conditions

I. Introduction

Pulmonary Diseases (PDs), also known as respiratory diseases, are diseases of the airways and the other structures of the lungs. PD is a disease that has many types under it that prevent the lungs from functioning properly. It can affect lung respiratory function, or the ability to breathe[1]. It is one of the world's most serious public health issues. This disease is a collection of chronic illnesses that damage the lungs' airways and other structures. It mostly affects the lungs and respiratory system [2].

Physicians used a variety of measures to distinguish between healthy and abnormal lung tissue anatomical structures, including intensity, shape, and texture[3]. However, due to the large amount of data collected by an X-ray image, it is a difficult task. As a result, the development of automatic Computerized Aid

Received: *July 26, 2023;* ***Revised****: 16 September 2023;* ***Accepted:*** *05 October 2023;* ***Published:*** *31 December 2023.*

Corresponding author- ***Minalu Chalie***

Diagnostic (CAD) tools is required to assist physicians in more properly analyzing and evaluating X-ray images.

The World Health Organization (WHO) reveals that pulmonary disease is one of the leading causes of increased mortality in humans [3]. To reduce the risk of high mortality rate to prevent respiratory diseases or illnesses appropriate treatment is required. Clinical examination is one of the methods used to diagnose various pulmonary diseases to save patients with appropriate treatments. The most common technique in clinical diagnosis is to use a CXR image to diagnose lung disease. In a clinical examination, the diagnosis is made by reading lung scan images. A highly skilled medical radiologist is required to read X-ray images of lung diseases or illnesses. However, this approach requires many medical professional workers to read scanned X-ray images.

The proposed method is based on the DCNN algorithm, which uses a group of neurons to convolve and extract significant characteristics from a given image. CNN is a neural network that uses the convolution operation as one of its layers[4]. Multiple convolutions and pooling layers may be present in a CNN, which is then followed by a fully connected network. This enables CNN to create a concept hierarchy in which more complex notions are built on simpler concepts. The notion is that the features are generated by a sequence of convolution and pooling layers, and the final classification function is learned by a normal neural network[5].

II. Related Works

Based on various experiments, Betsy Antony and Nizar Banu P. K. [6] investigated the detection of lung tuberculosis using methods such as filtering, segmentation, feature extraction, and classification. The researchers used a total of 662 X-ray images from the National Health Institute, 326 of which were normal and 336 of which were pulmonary tuberculosis. To remove unwanted noise from an image, a Gaussian filter and a median filtering technique were performed. The researchers used K-nearest neighbor, sequential minimal optimization, and simple linear regression models to detect whether pulmonary tuberculosis was represented or not. The classification accuracy in simple linear regression, sequential minimal optimization, and K-nearest neighbor is 79%, 75%, and 80% respectively.

Norval, Wang, and Sun [7] studied the accuracy of two methods for detecting tuberculosis based on CXR images of patients using CNN. Various image preprocessing methods have been developed to find the highest precision. A total of 406 normal images and 394 abnormal images were used in the simulation. They used X-ray equipment from Shenzhen Hospital and X-ray equipment from Montgomery County. Simulations show that the clipping region of interest plus the contrast enhancement produces excellent

Received: *July 26, 2023;* ***Revised****: 16 September 2023;* ***Accepted:*** *05 October 2023;* ***Published:*** *31 December 2023.*
Corresponding author- ***Minalu Chalie***

results. A hybrid method of combining primitive statistical CAD methods and neural networks has been studied. When the hybrid method is used to further enhance the image, better results can be obtained.

The researchers [8] studied the analysis of tuberculosis by DL with segmentation and augmentation of CXR. This study addresses the accuracy of the prediction of tuberculosis for relatively small datasets. The CNN was trained on the pre-processed dataset obtained after lung segmentation. The study [9], proposed based on preliminary results on pulmonary tuberculosis detection in chest X-ray using CNN. This study shows an experiment with a CNN architecture on public CXR databases to apply to diagnose pulmonary tuberculosis in chest X-ray images. As a consequence, depending on the network architecture, the study's AUC ranged from 0.78 to 0.84, sensitivity from 0.76 to 0.86, and specificity from 0.58 to 0.74.

The study [10], tried to simplify the diagnosis of pneumonia for professionals as well as for newcomers. The researchers recommend a novel DL framework for filtering using the concept of transfer learning to detect pneumonia. Another study [11], proposes a CNN model trained from scratch to detect and classify the presence of pneumonia from a collection of chest X-ray images. The researchers developed several data improvement algorithms to improve the image verification and classification accuracy of the CNN model and to enhance impressive verification accuracy.

Researchers [12] proposed a convolutional neural network for the classification of images and early diagnosis of pneumonia. For producing feature maps of the preprocessed X-ray image, they used a convolutional neural network technique. They found out that the accurate experimentation model classified the images with an accuracy of 85.73%. Ayan et al.[13], trained two classic CNN models, XceptionNet and VGG16Net, to use transfer learning and adjustment to classify images containing pneumonia. The accuracy results of the Vgg16 model and the XceptionNet model are 0.87% and 0.82% respectively.

Researchers in the study [6], surveyed state-of-the-art issues, and future directions that are used to provide deep learning of the lung's diagnosis in medical imaging. The paper is intended to provide an extensive survey of PD using deep learning, especially focusing on tuberculosis, pneumonia, and COVID-19. Another study [14], aimed to solve the problem of a lack of medical information regarding the work of diagnosing chest lung disease X-ray images using small data sets. In that study, the researchers combined two relatively small data sets of less than 103 images per class for classification images (detection of pneumonia and tuberculosis) and objectives of segmentation. In the best performance framework, researchers used network segmentation and InceptionV3 deep model classification.

Generally, several research works have been carried out in the area of respiratory disease recognition, but there are unexplored areas in binary classification (Pulmonary tuberculosis and pleural effusion) and ternary

Received: *July 26, 2023;* ***Revised****: 16 September 2023;* ***Accepted:*** *05 October 2023;* ***Published:*** *31 December 2023.*
Corresponding author- ***Minalu Chalie***

classification (pneumonia, pulmonary tuberculosis, and pleural effusion). In conclusion, the previous research works do not include the above classifications.

III. Materials and Methods

We discussed a detailed description of the proposed system structure for the detection and classification of PD. It is required to pass through a series of steps starting from the preprocessing of images, segmentation of the ROI, feature extraction, and learning to classify into predefined classes. The proposed research methodology architecture is depicted in Fig. 1.

A. Proposed System Architecture

The proposed system includes five main components: preprocessing, data augmentation, segmentation, feature extraction, and classification.

Received: *July 26, 2023;* ***Revised****: 16 September 2023;* ***Accepted:*** *05 October 2023;* ***Published:*** *31 December 2023.*
Corresponding author- ***Minalu Chalie***

ISSN (E): 2959-3921
(P): 2959-393X
DOI: https://doi.org/10.59122/144CFC16

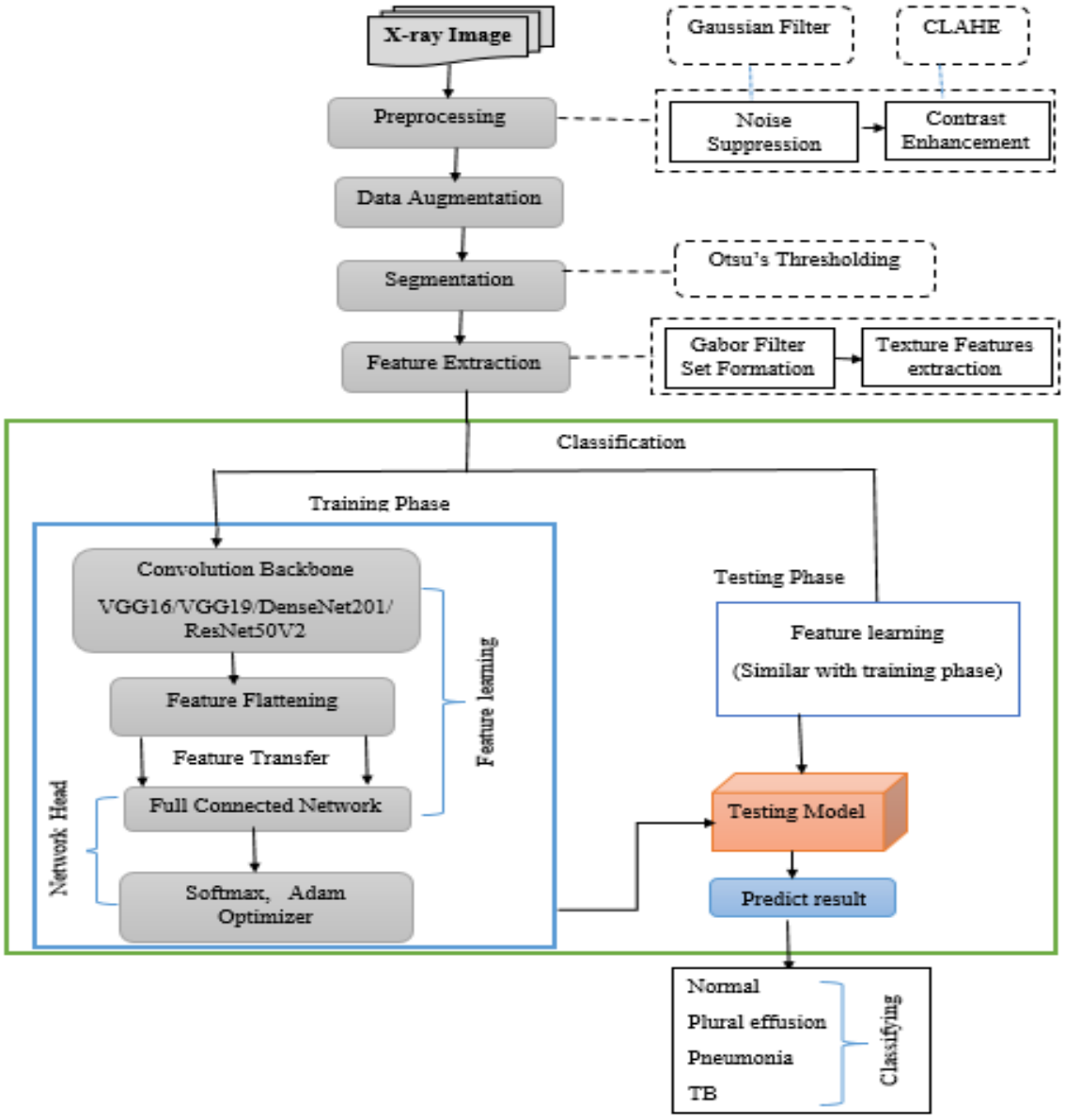

Fig. 1. Architecture of the proposed research methodology

B. Data Collection

Sample X-ray images are required to perform image processing operations on it. The researcher needs a lot of X-ray image samples to carry out this work. We collected chest X-ray images from Debre Markos Referral Hospital. In the image acquisition phase, normal and diseased images were taken. The sample data source contains representatives from each class type such as normal, pneumonia, pleural effusion, and pulmonary tuberculosis. A total of 1,019 X-ray images were collected in DICOM file format.

Received: *July 26, 2023;* ***Revised****: 16 September 2023;* ***Accepted:*** *05 October 2023;* ***Published:*** *31 December 2023.*

Corresponding author- ***Minalu Chalie***

ISSN (E): 2959-3921
(P): 2959-393X
DOI: https://doi.org/10.59122/144CFC16

Ethiopian International Journal of Engineering and Technology (EIJET)
Volume 1, Issue 2, 2023

The amount of collected X-ray image data was very small. When the amount of sampled dataset available is limited, some transformation is to be applied to the existing dataset to increase the amount of training sample set. As the size of training samples increased, the proposed system model was significantly improved. Due to the small size of our sample data source, we have increased data collection capacity using data augmentation techniques to improve system performance.

As a result, we increased our total data amount from 1019 to 2460 because this number has achieved the desired result for our system performance model. The training dataset consisted of 80% of the randomly selected images. The remaining 20% were used during testing, and their class distribution was labeled as normal, pneumonia, pleural effusion, and tuberculosis. During the model process, the training dataset was divided into a training set and a validation set using a 0.10 (10%) validation split.

C. *Preprocessing*

Pre-processing aims to improve the quality of the X-ray image so that the model analyzes it in a better way. In this process, we have smoothed or blurred the X-ray images to improve the quality of the X-ray image by enhancing unnecessary distorted features during image pre-processing.

1) Standardize images: In the preprocessing stage, the image size was resized to 224 x 224 pixels. Most advanced models [15] use the same image size as input, making it suitable for comparison. Using the same dimensions ensures consistency when evaluating our network against existing state-of-the-art models.

2) Adjust image quality: In this study, image smoothing was used to remove noise from the samples. Reducing noise to restore the original image is often a complex process. To address this, we applied the Gaussian Blur technique to clean the images. The Gaussian filter was implemented using the function cv2.GaussianBlur with a kernel size of 5x5.

The following function is used to calculate the Gaussian kernel [16]:

The two-dimensional image Gaussian filter equation is given by:

$$G(x,y) = \frac{1}{2\pi\sigma^2} e^{-\frac{x^2+y^2}{2\sigma^2}} \quad (1)$$

Where σ is the standard deviation of the distribution containing the x and y coordinates in two-dimensional images.

3) Contrast enhancement: As depicted in Fig. 2, we used histogram equalization in this study to increase image contrast enhancements by enhancing the brightness difference between lung objects and their

Received: *July 26, 2023;* ***Revised****: 16 September 2023;* ***Accepted:*** *05 October 2023;* ***Published:*** *31 December 2023.*
Corresponding author- ***Minalu Chalie***

ISSN (E): 2959-3921
(P): 2959-393X
DOI: https://doi.org/10.59122/144CFC16

backgrounds. There are two advanced histogram equalization techniques: these are Adaptive Histogram Equalization (AHE) and Contrasted Limited Adaptive Histogram Equalization (CLAHE).

CLAHE has been used to improve the contrast of X-ray medical images. The contrast limitation of CLAHE distinguishes it from typical AHE. The CLAHE technique divides an input original image into non-overlapping contextual parts known as sub-images, tiles, or blocks. There are two parameters in CLAHE: block size and clip limit, which are used to control image quality. The CLAHE method applied histogram equalization to each region of the X-ray image context. The clipped pixels are redistributed over each grey level, and the original histogram is cropped [17]. In the redistributed histogram, the intensity of each pixel is limited to a fixed maximum value, unlike in a standard histogram.

After using the CLAHE method, we obtained improved X-ray images. The enhanced image was obtained by creating a histogram equalization mapping for all pixels. Improving contrast enhancement shows differences in image brightness. During the histogram equalization mapping process, this study used clip Limit 2.0 and tile Grid Size (2, 2). These two parameters are used to improve X-ray image brightness as shown in the image below, Fig.2.

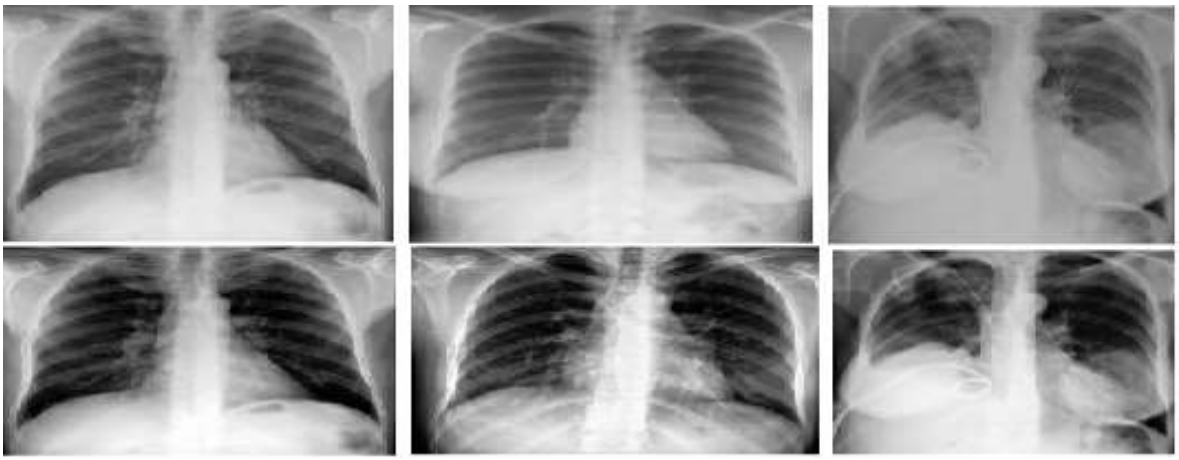

Fig. 2. Effect of CLAHE (below) on the blurred input image

D. Data Augmentation

We used data augmentation techniques on the X-ray image dataset to increase the number of useful images and improve the diversity of the dataset. Data augmentation techniques have different criteria to make different identical content such as rotation range, horizontal shift, vertical shift, shear range, zoom range, and horizontal flip. We have used the above criteria in data augmentation operation to increase the size of our data sets. In our situation, we rotated our input images by 10 degrees at random. The random rotations' degree range is controlled by a 10-degree rotation range. We also used the horizontal transformation of the images by 0.2 percent, and a vertical transformation of the images by 0.2 percent, which is called the width

Received: *July 26, 2023;* ***Revised****: 16 September 2023;* ***Accepted:*** *05 October 2023;* ***Published:*** *31 December 2023.*
Corresponding author- ***Minalu Chalie***

ISSN (E): 2959-3921
(P): 2959-393X
DOI: https://doi.org/10.59122/144CFC16

and height shift respectively. In addition, the image angles are clipped in a counterclockwise direction by a shear range of 0.2 percent. The shear range controls the angle in an anti-clockwise direction as a radian in which our input image is allowed to be sheared. The image was then flipped horizontally after the zoom range was randomly zoomed to a ratio of 0.2 percent.

E. Segmentation

Image segmentation is well known for allowing the splitting of an image into targeted image objects or segments that appear as distinct categories of pixels, with each category becoming a segment. In this study, we used Otsu's thresholding technique, which has been widely reported to yield interesting findings. It is important to distinguish between ROI and other image regions. This technique allows for automatically computing the optimum threshold value from the input image[18].

So far, we have used a 5x5 Gaussian kernel to eliminate noise from our image samples, followed by Otsu thresholding. As a result, threshold segmentation was used to divide the image into the area of interest and another region. The main work is to separate the image histogram into two clusters by minimizing the weighted variance of these classes denoted by $\sigma_{\omega}^{2}(t)$. The total computation equation is described as follows: -

$$\sigma_{\omega}^{2}(t)=\omega 1(t)\sigma_{1}^{2}(t)+\omega 2(t)\sigma_{2}^{2}(t) \quad (2)$$

$\omega 1(t)$, $\omega 2(t)$ are the probabilities of the two classes divided by threshold t, with values ranging from 0 to 255. There are two options for finding thresholding. The first is to minimize the class variance described in the above $\sigma_{\omega}^{2}(t)$ and the second is to maximize the variance between classes by using the following expression. The variance between classes is defined as[19]:-

$$\alpha_{b}^{2}(t)=\omega 1(t)\omega 2(t)\,(\mu_{1}(t)-\mu_{2}(t))^{2} \quad (3)$$

$$\alpha_{T}^{2}=\alpha_{b}^{2}(t)+\sigma_{\omega}^{2}(t) \quad (4)$$

Where α_{T}^{2} and μ are the total variance of the image and the mean of the class, respectively. As shown in Fig.3, when we applied the Otsu method to the raw image, we obtained the ROI result on the image.

Fig. 3. ROI Segmentation

Received: *July 26, 2023;* ***Revised****: 16 September 2023;* ***Accepted:*** *05 October 2023;* ***Published:*** *31 December 2023.*
Corresponding author- ***Minalu Chalie***

ISSN (E): 2959-3921
(P): 2959-393X
DOI: https://doi.org/10.59122/144CFC16

F. Feature Extraction

The structure of a human lung is interesting, and it holds a lot of textural information. It has distinguishing textural features that are used to determine whether a person is infected or not. We have used the Gabor filter technique to extract features of the X-ray images. Gabor filters have long been popular in computer vision, particularly for texture analysis. Textural properties in images can be utilized to detect lung illnesses accurately. The Gabor filter is one of the most widely used techniques for extracting or analyzing texture features[20]. A collection of Gabor filters with varying frequencies is used to extract textural characteristics from the image.

As depicted in Fig.4, when we apply a Gabor filter on raw images, the textures on the image are easily visible and easy to identify and classify for lung disease for the CNN model.

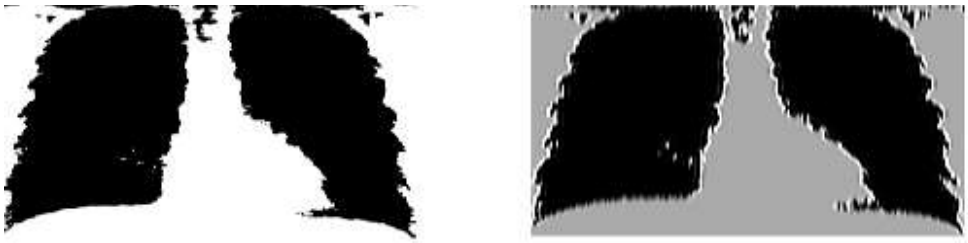

Fig. 4: Left: raw image right: image on the left applied with Gabor filter

G. Classification

Classification is the final task of this work. As we discussed in the literature review, there are different algorithms used for classification purposes. In this study, we selected VGG16, VGG19, ResNet50V2, and DensNet201 classifiers with SoftMax activation functions for classification. The reason we chose these classic learning models is based on popularity as they are now highly rated for feature extraction and classification. Classification is done by using the knowledge from the learning model, which is constructed by using the training and testing phases. In the training phase, the training dataset is used. By using the knowledge from the learning model, we categorize each image (in the testing dataset) into a specific or predefined class (normal, pneumonia, pulmonary tuberculosis, and pleural effusion).

IV. Experimental Setup and Result Analysis

A. Experimental setup

We defined several system hyperparameters and selected their values carefully based on experimental results. Designing and developing a high-performing system model is a critical task. The performance of the system depends largely on the choice of network parameters. Since many hyperparameters need to be tested at each stage, we identified the best values for each one in network architecture. In the proposed

Received: *July 26, 2023;* ***Revised****: 16 September 2023;* ***Accepted:*** *05 October 2023;* ***Published:*** *31 December 2023.*
Corresponding author- ***Minalu Chalie***

system, different parameter combinations were tested, and the model with the lowest loss or error rate was chosen.

We have been feeding neural network training data throughout epoch 30. We got a better fit when we fed it a new "unseen" input (test data). After training our model using epoch 30, we got optimal model performance. Our network was trained with Adam Optimizer. Adam is one of the deep neural network training optimizers that uses an adaptive learning rate optimization mechanism. We used the ReLU activation function. For multiclass classification tasks, the SoftMax function is utilized. We have developed a network or model for four-class classification, and the network's output layer has the same number of neurons as the target's number of classes. For this reason, we used the SoftMax activation function for pulmonary disease classification to improve performance and computational time.

B. Models

The models were expanded with feature flattening, a fully connected layer having 512 and 256 neurons, dropout, and a SoftMax classifier. When we chose and used this neuron, we achieved the highest accuracy according to our goals. When measuring network performance, we found a good representation of our test goals using metrics. The deep neural networks had a total of 6,423,812 trainable parameters for VGG16, 25,695,236 for VGG19, 51,382,788 for ResNet50V2, and 48,171,524 DenseNet201. Before feeding the input images into deep neural networks used for feature extraction, all image batches were adjusted to match the same format (batch size, input scale, etc.) as those used in the trained models. During training, our neural network classifiers learned bias and weight parameters by backpropagating errors to minimize categorical cross-entropy using the Adam optimizer.

The models were later validated using different sets of hyper-parameters observed during the training process. The SoftMax classifier produces a vector of probabilities indicating whether or not an input image belongs to one of the classes. The final class is the one that corresponds to the highest value, and its position is then mapped back to a class.

The model is trained on 30 epochs, a batch size of 32 and 64, and a starting or initial learning rate of 0.001 (1e-3). The data is partitioned into a training and testing dataset, which means that the training dataset is used to train the model, and the test dataset is assigned to test the performance of the model.

C. Results

We have used precision, recall, and F1-score to measure the performance of our model. We showed the performance of our model by applying the Gabor filter. The training phase is the sequence of feature flattening, activation function, and fully connected layers and dropout after the final fully connected layers

Received: *July 26, 2023;* ***Revised****: 16 September 2023;* ***Accepted:*** *05 October 2023;* ***Published:*** *31 December 2023.*
Corresponding author- ***Minalu Chalie***

ISSN (E): 2959-3921
(P): 2959-393X
DOI: https://doi.org/10.59122/144CFC16

and before the SoftMax classifier. The training process was then stopped, and the final results were measured as an average of all results obtained at that step. The final step was to demonstrate the performance of selected models on previously unknown data (test set).

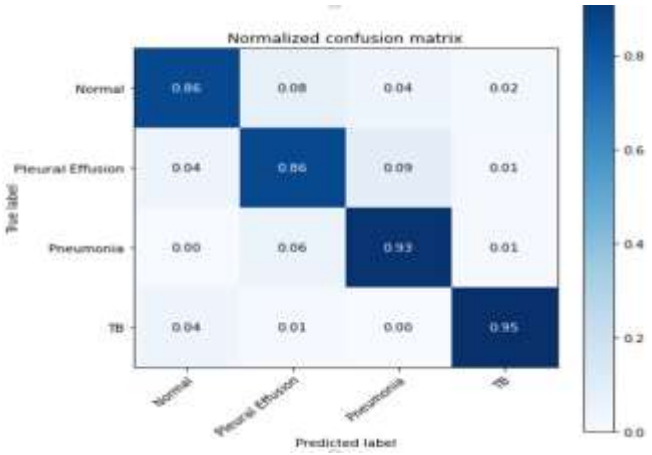

	precision	recall	f1-score	support
Normal	0.91	0.85	0.88	123
Pleural Effusion	0.86	0.85	0.85	123
Pneumonia	0.88	0.92	0.90	123
TB	0.97	0.95	0.96	123
micro avg	0.91	0.89	0.90	492
macro avg	0.91	0.89	0.90	492
weighted avg	0.91	0.89	0.90	492

Fig. 5. Confusion matrix and classification accuracy VGG16 model on batch size 64

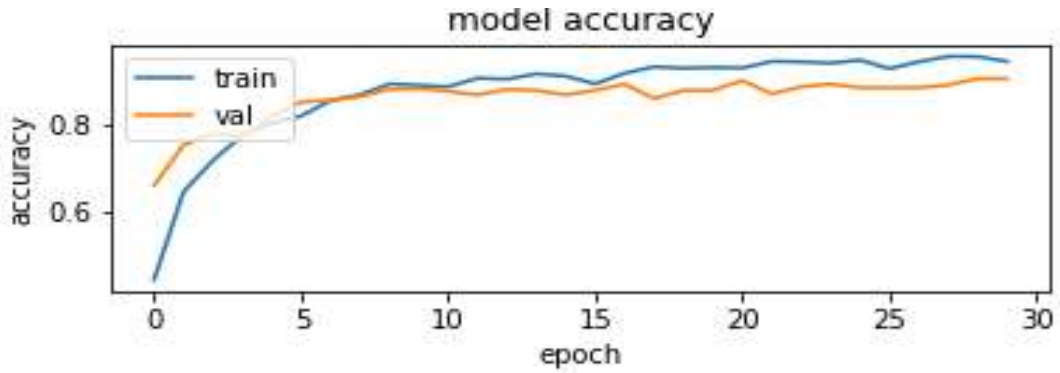

Fig. 6. Training and validation accuracy curve of VGG16 on batch size 64

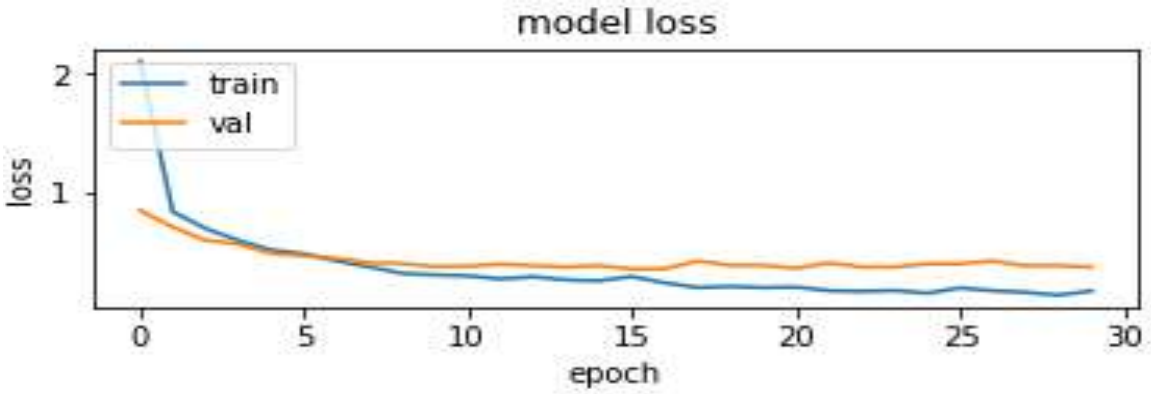

Fig. 7: Training and validation loss curve of VGG16 on batch size 64

Received: *July 26, 2023;* ***Revised****: 16 September 2023;* ***Accepted:*** *05 October 2023;* ***Published:*** *31 December 2023.*

Corresponding author- ***Minalu Chalie***

Table I: Experimental Test Result

Model	Epoch	Learning rate	Optimizer	Batch Size	Training Accuracy (%)	Test Accuracy (%)	Loss Accuracy (%)	Model size (in MB)
VGG16	30	0.001	Adam	32	92.21	90.04	43.31	4.6
				64	94.12	90.24	36.14	4.6
VGG19	30	0.001	Adam	32	96.65	90.24	37.87	25.69
				64	97.47	92.07	30.26	25.69
ResNet50V2	30	0.001	Adam	32	95.05	94.31	24.93	51.38
				64	96.82	94.51	33.08	51.38
DenseNet201	30	0.001	Adam	32	95.65	95.12	19.01	48.17
				64	97.80	95.73	16.92	48.17

V. Discussion

Experimental results of the proposed model for automatic detection and classification of PD are described in detail hereunder. The dataset used and the implementation of the proposed model are described briefly. We have developed four deep CNN models, which are VGG16, VGG19, ResNet50v2, and DensNet201. These models were trained using the same epoch, learning rate, and optimizer. We have defined the experimental result for each model. For each model as depicted in Fig. 5, 6, and 7, we described in detail the confusion matrix, classification report, accuracy, and loss curve.

The models are trained using the same image size. In these trained models, we used standard image sizes (224,224). We have evaluated the performance of our model by comparing its performance with the state-of-the-art models. To begin with, using two different batch sizes, we showed the performance of the models. We trained models using two different batch sizes: 32 and 64. When we changed the size of the batch, our model performances showed a little difference in training accuracy and test accuracy. As shown in Table I above, the trained models in batch size 64 performed better than those in batch size 32. In addition, comparisons of the models are performed based on accuracy, loss, and size of parameters. In terms of size, the training is better to train the model quickly on a small size (small number of parameters). The VGG16 model has a small number of parameters, so it is better to train the model. However, this model has high validation loss and smaller test accuracy compared to the other models. As a result, VGG16 has made the computational resources especially those used in memory more efficient. Based on the accuracy of the model, the DenseNet201 model has achieved a higher accuracy for the detection and classification of diseases. The experiment result of the DenseNet201 model trained in a batch size of 32 achieved 95.65% training accuracy and 95.12% testing accuracy. As well, the experiment result of the DenseNet201 model

Received: *July 26, 2023;* ***Revised****: 16 September 2023;* ***Accepted:*** *05 October 2023;* ***Published:*** *31 December 2023.*
Corresponding author- ***Minalu Chalie***

trained in batch size 64 achieved 97.80% training accuracy and 95.73% testing accuracy. The DenseNet201 model trained on a batch size of 64 has a low validation loss value (16.92%), making it better for classifying pulmonary disease cases.

Generally, the DenseNet201 model ensured the best result without overfitting or underfitting problems. The result of the DenseNet201 model did not show much difference in terms of training and testing accuracy. The DenseNet201 model has higher classification accuracy than VGG16, VGG19, and ResNet50V2. Therefore, the DenseNet201 model is better for finding new pulmonary disease cases.

VI. Conclusion

In this study, we focused on exploring lung disease classification problems using deep neural networks. A deep CNN model was developed for the detection and classification of PD using images of both normal and infected lungs. We used Gabor filter techniques before the DCNN algorithm to improve our model performance. The Gabor filter technique is used for textural features to determine whether a person is infected or not. The textural features in images are used to detect lung illnesses accurately. As a result, the use of the Gabor filter has made our model's performance better.

The significance of the developed system has changed in the progress of diagnosis in terms of accuracy and efficiency. The CXR images were used in the proposed method to separate four classes into normal, pneumonia, pulmonary tuberculosis, and pleural effusion. We also compared our proposed deep CNN with other neural learning networks (Including VGG16, VGG19, ResNet50V2, and DensNet201). The model results are summarized in Table I, in which we used accuracy to evaluate the performance since the test dataset in the class was equally distributed. In our models, the DenseNet201 proposed model has achieved better results in terms of accuracy and loss. In terms of accuracy, we have 97.80% training accuracy and 95.73% testing accuracy which are far above state-of-the-art models. So, the DenseNet201 model that records higher accuracy is better for detecting and classification of pulmonary diseases. Due to the good performance of the proposed algorithm, it can be used as a smart computer assistant in the field of medicine for rapid diagnosis.

REFERENCES

1. J. L. López-Campos, J. J. Soler-Cataluña, and M. Miravitlles, “Global strategy for the diagnosis, management, and prevention of chronic obstructive lung disease 2019 report: future challenges,” *Arch. Bronconeumol.*, vol. 56, no. 2, pp. 65–67, 2020.
2. M. Varmaghani, M. Dehghani, E. Heidari, F. Sharifi, S. S. Moghaddam, and F. Farzadfar, “Global prevalence of chronic obstructive pulmonary disease: Systematic review and meta-analysis,” *East. Mediterr. Heal. J.*, vol. 25, no. 1, pp. 47–57, 2019, doi: 10.26719/emhj.18.014.

Received: *July 26, 2023;* ***Revised****: 16 September 2023;* ***Accepted:*** *05 October 2023;* ***Published:*** *31 December 2023.*
Corresponding author- ***Minalu Chalie***

3. J. Y. Choi et al., "Comparison of clinical characteristics between chronic bronchitis and non-chronic bronchitis in patients with chronic obstructive pulmonary disease," *BMC Pulm. Med*., vol. 22, no. 1, pp. 1–9, 2022, doi: 10.1186/s12890-022-01854-x.
4. M. A. Wani, F. A. Bhat, S. Afzal, and A. I. Khan, "Introduction to Deep Learning," in *Advances in Deep Learning*, M. A. Wani, F. A. Bhat, S. Afzal and A. I. Khan, Eds., Gateway East, Singapore: Springer, 2020, pp. 1–11. doi: 10.1007/978-981-13-6794-6_1.
5. J. Wu, *Introduction to Convolutional Neural Networks*, Nanjing University, China: LAMDA Group National Key Lab for Novel Software Technology, May 1, 2017, pp. 1–31.
6. S. T. H. Kieu, A. Bade, M. H. A. Hijazi, and H. Kolivand, "A survey of deep learning for lung disease detection on medical images: State-of-the-art, taxonomy, issues, and future directions," *J. Imaging*, vol. 6, no. 12, p. 131, 2020, doi: 10.3390/jimaging6120131.
7. M. Norval, Z. Wang, and Y. Sun, "Pulmonary tuberculosis detection using deep learning convolutional neural networks," 3rd *ACM Int. Conf. Proceedings Ser*., October 2020, pp. 47–51, 2019, doi: 10.1145/3376067.3376068.
8. S. Stirenko et al., "Chest X-ray analysis of tuberculosis by deep learning with segmentation and augmentation," *arXiv, 2018 IEEE 38th International Conference on Electronics and Nanotechnology (ELNANO)*, Kiev, 2018, pp. 422-428.
9. M. E. Colombo Filho et al., "Preliminary results on pulmonary tuberculosis detection in chest x-ray using convolutional neural networks," *Computational Science – ICCS 202020th International Conference*, Proceedings, *Part IV* Amsterdam, The Netherlands: PMCID: PMC7303695, June 3–5, 2020, 12140, pp. 563-576
10. V. Chouhan et al., "A novel transfer learning based approach for pneumonia detection in chest X-ray images," *Appl. Sci*., vol. 10, no. 2, 2020, doi: 10.3390/app10020559.
11. T. Gao, "Chest X-ray image analysis and classification for COVID-19 pneumonia detection using deep CNN," medRxiv, pp. 1–14, 2020, (Preprint) doi: 10.1101/2020.08.20.20178913.
12. H. Magar, S. J. Patil, S. R. Waykole, S. D. Sandikar, and N. D. Parakh, "Pneumonia detection using x-ray images with deep learning," *Inter. J. of Comp. Appl. Tech. and Research* vol. 9, no. 5, pp. 183–185, 2020.
13. E. Ayan and H. M. Ünver, "Diagnosis of pneumonia from chest X-ray images using deep learning," *Sci. Meet. Electr. Biomed. Eng. Comput. Sci*. EBBT 2019, pp. 0–4, 2019
14. M. Zak and A. Krzyżak, "Classification of lung diseases using deep learning models," *Computational Science – ICCS 2020*, 12139 LNCS, pp. 621–634, 2020.
15. M. B. Jerubbaal John Luke, Rajkumar Joseph and Cognitive, "Impact of image size on accuracy and

Received: *July 26, 2023;* ***Revised****: 16 September 2023;* ***Accepted:*** *05 October 2023;* ***Published:*** *31 December 2023.*
Corresponding author- ***Minalu Chalie***

generalisation of convolutional neural networks," *Int. J. Res. Anal. Rev.*, vol. 6, no. 1, 2019.

16. A. Padmanabhan and S. Dinesh, "The effect of Gaussian blurring on the extraction of peaks and pits from digital elevation models," *Discrete. Dyn. Nat. Soc.*, vol. 2007, no. 1, 2007.
17. J. Ma, X. Fan, S. X. Yang, X. Zhang, and X. Zhu, "Contrast Limited Adaptive Histogram Equalization Based Fusion for Underwater Image Enhancement," no. March, pp. 1–27, Preprints 2017, 2017030086. https://doi.org/10.20944/preprints201703.0086.v1.
18. J. Yousefi, "Image Binarization using Otsu Thresholding Algorithm," Guelph, ON, Canada: University of Guelph, April 2011. https://www.researchgate.net/profile/Jamileh-Yousefi 2/ publication /277076039 _Image_Binarization_using_Otsu_Thresholding_Algorithm/links/55609b1408ae8c0cab31ea42/Image-Binarization-using-Otsu-Thresholding-Algorithm.pdf
19. A. Kumar and A. Tiwari, "A comparative study of Otsu thresholding and K-means algorithm of image segmentation," *Int. J. Eng. Tech. Res*., vol. 9, no. 5, pp. 12–14, 2019.
20. Y. Wicaksono and V. Suhartono, "Color and texture feature extraction using Gabor filter," *J. Intell. Syst*., vol. 1, no. 1, pp. 15–21, 2015.

Received: *July 26, 2023;* ***Revised****: 16 September 2023;* ***Accepted:*** *05 October 2023;* ***Published:*** *31 December 2023.*
Corresponding author- ***Minalu Chalie***